# Involvement of the orphan nuclear estrogen receptor-related receptor α in osteoclast adhesion and transmigration

## Edith Bonnelye[1,2], Frédéric Saltel[1*†], Anne Chabadel[1*], Ralph A Zirngibl[3], Jane E Aubin[3] and Pierre Jurdic[1]

[1]Institut de Génomique Fonctionnelle de Lyon, Université de Lyon, Université Lyon 1, CNRS, INRA, Ecole Normale Supérieure de Lyon, 69007 Lyon, France

[2]INSERM U664, Faculté de Médecine RTH Laennec, Rue Guillaume Paradin, 69372 Lyon Cedex 08, France

[3]Department of Molecular Genetics, Medical Sciences Building, 1 King's College Circle, Toronto, Ontario, Canada M5S 1A8

(Correspondence should be addressed to E Bonnelye at INSERM U664, Faculté de Médecine RTH Laennec; Email: edith.bonnelye@inserm.fr)

*(F Saltel and A Chabadel contributed equally to this work)

†(F Saltel is now at European Institute of Chemistry and Biology, Unité INSERM 889, Université Victor Segalen Bordeaux 2, IFR66, 2, rue Robert Escarpit, 33 600 Pessac, France)

## Abstract

The orphan nuclear receptor, estrogen receptor-related receptor α (ERRα) is expressed in osteoblasts and osteoclasts (OCs) and has been proposed to be a modulator of estrogen signaling. To determine the role of ERRα in OC biology, we knocked down ERRα activity by transient transfection of an siRNA directed against ERRα in the RAW264.7 monocyte–macrophage cell line that differentiates into OCs in the presence of receptor activator of nuclear factor κB-ligands and macrophage colony-stimulating factor. In parallel, stable RAW cell lines expressing a dominant-negative form of ERRα and green fluorescent protein (RAW-GFP-ERRαΔAF2) were used. Expression of OC markers was assessed by real-time PCR, and adhesion and transmigration tests were performed. Actin cytoskeletal organization was visualized using confocal microscopy. We found that RAW264.7 cells expressing siRNA directed against ERRα and RAW-GFP-ERRαΔAF2 OCs displayed abnormal spreading, and decreased osteopontin and β3 integrin subunit expression compared with the corresponding control cells. Decreased adhesion and the absence of podosome belts concomitant with abnormal localization of c-src were also observed in RAW-GFP-ERRαΔAF2-derived OCs. In addition, RAW-GFP-ERRαΔAF2-derived OCs failed to transmigrate through osteoblast cell layers. Our data show that the impairment of ERRα function does not alter OC precursor proliferation and differentiation but does alter the adhesion/spreading and migration capacities of mature OCs.

*Journal of Molecular Endocrinology* (2010) **45**, 365–377

## Introduction

Osteoclasts (OCs) are large multinucleated cells of hematopoietic origin formed by the differentiation and fusion of mononuclear monocyte–macrophage lineage precursors after stimulation by receptor activator of nuclear factor κB-ligands (RANKL) and macrophage colony-stimulating factors (M-CSF; Boyle *et al.* 2003). OC formation is associated with the expression of markers such as tartrate-resistant acid phosphatase (TRAP) and calcitonin receptor (CTR). Moreover, OCs are highly polarized cells, and several studies have identified a series of factors involved in OC spreading, polarity, adhesion, and migration, such as osteopontin (OPN), integrin subunits αv, β1, β3, β5, cluster of differentiation 44 (CD44), c-src, and tumor necrosis factor receptor-associated factor 6 (Traf6; Denhardt & Noda 1998, Chellaiah & Hruska 2003, Chabadel *et al.* 2007, Teitelbaum 2007). OCs are highly migratory on bone surfaces or through collagen (Domon *et al.* 2002, Delaisse *et al.* 2003, Saltel *et al.* 2004). Recently, we have found that OCs are also able to transmigrate through cell layers, a process that involves c-src and metalloproteinases (MMPs; Saltel *et al.* 2006). Moreover, OCs exhibit several features, such as podosomes, that are associated with cell adhesion, migration, and invasion. In fact, we have previously shown that mature OCs, when spread on glass or plastic, form highly dynamic podosome belts (Destaing *et al.* 2003, Jurdic *et al.* 2006) at their periphery; whereas, when cultured on apatite mineral (corresponding to the mineral phase of bone), they exhibit another actin-rich structure, the sealing zone, which seals off the resorption area (Vaananen *et al.* 2000, Saltel *et al.* 2004, 2008).

Nuclear steroid receptors are transcription factors involved in various physiological regulatory processes, including multiple processes in bone (Gennari *et al.* 2007). The superfamily to which nuclear receptors belong comprises both ligand-dependent molecules such as ERs and a large number of so-called orphan

receptors, for which no ligands have yet been determined (Benoit *et al.* 2006). Three orphan receptors, ER-related receptor α (ERRα), ERRβ, and ERRγ (NR3B1, NR3B2, and NR3B3 respectively, according to the Nuclear Receptors Nomenclature Committee 1999), share similarities with ERα and ERβ (NR3A1 and NR3A2 respectively; Green *et al.* 1986, Kuiper *et al.* 1996), but they do not bind estrogen (Greschik *et al.* 2002, Kallen *et al.* 2004). Sequence alignment of ERRα and the ERs reveals a high similarity (68%) in the 66 amino acids (aa) of the DNA-binding domain, but only a moderate similarity (36%) in the ligand-binding domain, which may explain the fact that ERRα recognizes the same DNA-binding elements as ERs but does not bind estrogen (Giguere *et al.* 1988). Several studies have shown that ERRα may activate gene transcription constitutively essentially through its coactivator-binding domain AF-2 (Vanacker *et al.* 1999, Kallen *et al.* 2004). ERRα regulates fatty acid oxidation and the adaptative bioenergetic response (Luo *et al.* 2003, Huss *et al.* 2007). ERRα is highly expressed in skeletal (bone and cartilage) tissues (Bonnelye *et al.* 2001, 2007) and has been reported to regulate osteoblast development and bone formation *in vitro* (Bonnelye *et al.* 2001, 2007) and *in vivo* (Delhon *et al.* 2009, Teyssier *et al.* 2009). One study out of two has also described an *ESRRA* gene regulatory variant that is associated with bone mineral density and index in premenopausal women (Laflamme *et al.* 2005, Giroux *et al.* 2008).

In addition to its expression in osteoblasts, we have previously described ERRα expression in multinucleated TRAP-positive OCs in rat femurs after ovariectomy (Bonnelye *et al.* 2002). We therefore decided to address the possible function of ERRα in osteoclastogenesis, including OC differentiation and adhesion–transmigration activities, using RAW264.7 cells transfected with an siRNA directed against ERRα or with a wild-type (WT) or a dominant-negative form of ERRα.

## Materials and methods

### Reagents

A pEGFP vector (Clontech) was used to obtain the stable RAW-GFP(Ct) and RAW-GFP-ERRαΔAF2 (clones 1, 2, and 3) cell lines. Mouse ERRα cDNA (WT and ΔAF2) was obtained from mRNA extracted from primary OCs derived from spleen cells on day 6, using reverse transcription (RT)-PCR with specific primers ((NM_007953.1): ERRα upstream (177 bp): TCC AGC ACC ATG TCC AGC; ERRα downstream (WT) (1–1436 bp): CCA CCC CTT GCC TCA GTC CAT; ERRα downstream (ΔAF2): TCA TGC TGT CTG GCG GA (1–1341 bp); helix 11–12 deletion (42 aa);

Bonnelye *et al.* 2007). Amplicons were sequenced for verification. Anti-phospho-src (pTyr418) was from Abcam (ab4816); anti-integrin β3 chain was from BD (San Jose, CA, USA); anti-GFP was from Roche (monoclonal antibody mixture, clones 7.1 and 13.1). CY5-conjugated secondary antibodies (anti-rabbit, -mouse, -goat, and -hamster; 1/3000 final dilution) were from Jackson ImmunoResearch Laboratories (West Grove, PA, USA). The F-actin distribution was revealed with Alexa Fluor-546-Phalloidin from Molecular Probes (Eugene, OR, USA).

### Cell culture

MC3T3-E1 cells were cultured in α-MEM containing 10% fetal bovine serum (FBS; Zirngibl *et al.* 2008). On the day of transfection, cells were transfected using Lipofectamine 2000 (Invitrogen). Spleen cells from 6-week-old OF1 male mice, none modified RAW264.7 and RAW264.7 (GFP(Ct) and GFP-ΔAF2) cells were cultured for 8 and 6 days respectively in differentiation medium: α-MEM containing 10% FCS (BioWest, Nuaille, France), 20 ng/ml M-CSF and 20 ng/ml soluble recombinant RANKL (Destaing *et al.* 2003).

### RNA interference (siRNA)

The ERRα siRNA sequence was GCU AGU GCU CAG CUC UCU ACC CAA (403–426 bp) (Invitrogen). This sequence was rigorously analyzed by BLAST search, and no homologies were found; this included no homology with any of the ERα, ERβ, ERRβ, or ERRγ, or with any other currently known nuclear receptors. The recommended negative control (Sc) by the manufacturer was used (Medium GC stealth RNA interference negative control duplexes; Invitrogen). ERRα siRNA and Sc were transfected twice into RAW cells following the manufacturer's protocol on days 3 and 4 after the addition of RANKL. mRNA was extracted on day 5.

### Transactivation assay

HeLa cells were plated at 40 000 cells/well on a 24-well plate in DMEM (Sigma D5796) plus 10% FBS the day before transfection and incubated in a humidified incubator at 37 °C in a 95% air–5% $CO_2$ atmosphere. Media were changed just prior to transfection and again 24 h after transfection. Cells were transfected with Lipofectamine 2000 (Invitrogen) following the manufacturer's protocol using 100 ng expression vector, 200 ng luciferase reporter vector, and 10 ng pRL tk luc (Promega) for normalization. The pGL3 BSP reporter contains the rat bone sialoprotein promoter from −448 to −1 relative to the transcription start site cloned into pGL3B (Promega). Luciferase activities

were measured 48 h later on an EG&G Berthold Microplate Luminometer LB96V (EG&G Berthold GmbH & Co., Oak Ridge, TN, USA) using the Dual-Luciferase reporter assay system (Promega). Transfections were repeated at least three times, and a representative experiment is shown.

## Osteoclast differentiation and spreading test

After 6 days, GFP(Ct) and GFP-ΔAF2 (1, 2, and 3) cells were fixed with paraformaldehyde (PFA; Merck), then stained for TRAP using a histochemical kit (no. 387; Sigma–Aldrich), following the manufacturer's instructions. Multinucleated TRAP-positive cells containing three or more nuclei were counted as OCs. To quantify OCs spreading, OCs derived from GFP(Ct) and GFP-ΔAF2 (1, 2, and 3) cells were fixed and labeled with Alexa Fluor-546-Phalloidin to visualize, by fluorescence, specific F-actin structure-containing podosome belts that characterize spread OCs. Spread OCs were quantified by counting the podosome belts versus the total number of OCs, under a X40 (NA 1.0) Zeiss Plan-Achromat objective and expressed as percentage. Results were plotted as the mean percentage of podosome belt number ±s.D. of triplicate wells for GFP(Ct)- and GFP-ΔAF2 (1, 2, and 3)-derived OCs and for siRNA-transfected cells and are representative of two independent experiments each.

## Adhesion test

OCs were detached and re-seeded on plastic in 12-well plates. The OCs were incubated at 37 °C in PBS containing 0·25 mM EDTA (PBS–EDTA) 4 h later. The incubation was stopped either immediately ($T=0$) or after 35 min ($T=35$). Cultures were then fixed with PFA and stained for TRAP. Adhesion was quantified by counting OCs that were still adherent at $T=35$ min versus the total number of OCs at $T=0$ and expressed as percentage. Results were plotted as the mean percentage of adherent OCs±s.D. of triplicate wells for GFP(Ct)- and GFP-ΔAF2 (1, 2, and 3)-derived OCs and are representative of two independent experiments.

## Transmigration assay

A transmigrating OC is an OC that had been detached and re-seeded on cell multilayers (for instance, osteoblasts) and that in 12 h is able to cross the osteoblast multilayers without destroying them and to spread on the plastic substratum beneath the osteoblast. We used the osteoblastic cell line MC3T3-E1, which we cultured for at least 1 week to obtain multilayers of osteoblasts. At the end of the OC

differentiation process, OCs derived from GFP(Ct) and GFP-ΔAF2 (1, 2, and 3) were removed and re-seeded on the top of the multilayers of MC3T3-E1 cells as described previously (Saltel *et al.* 2006). Primary OCs were also treated with echistatin at $10^{-8}$ M (Sigma–Aldrich) for 24 h, then seeded on MC3T3 in the presence of echistatin at $10^{-8}$ M for 12 h. Cells were then fixed after 20 min or 12 h, then permeabilized with 0·2% Triton X-100 for 7 min, and stained with Alexa Fluor-546-Phalloidin. OC transmigration efficiency was quantified using a X40 (NA 1.0) Zeiss Plan-Achromat objective by counting the transmigrated OCs versus the total number of OCs and expressed as percentage. Results were plotted as the mean of the number of the transmigrated OCs±s.D. of three wells for GFP(Ct)- and GFP-ΔAF2 (1, 2, and 3)-derived OCs and as the mean number of the transmigrated OCs± s.D. of three wells for non-treated OCs and OCs treated with echistatin. They are representative of three and two independent experiments respectively.

## RT-PCR

Total RNA was extracted with TRIzol reagent from OC derived from spleen cells and RAW cells (GFP(Ct) and GFP-ΔAF2 (1, 2, and 3)) and from siRNA-transfected RAW cells. Samples of total RNA were reverse-transcribed using SuperScript II retrotranscription kit (Invitrogen; Bonnelye *et al.* 2001). Semi-quantitative PCR was performed for all studied genes. Real-time PCR was carried out to confirm regulated genes found by semi-quantitative PCR. Real-time RT-PCR was carried out by using the LightCycler system (SYBR Green; Qiagen) according to the manufacturer's instructions. PCRs were performed with the primers listed in Table 1, and amplimers were all normalized to corresponding L32 values. Data normalization: in real-time PCR, each replicate average gene's $C_T$ was normalized to the average $C_T$ of L32 by subtracting the average $C_T$ of L32 from each replicate to give the $\Delta C_T$. Results are expressed as Log$^{-2\Delta\Delta C_T}$ with $\Delta\Delta C_T$ equivalent to the $\Delta C_T$ of the genes in GFP-ΔAF2 (1, 2, and 3) or siRNA subtracting to the $\Delta C_T$ of the endogenous control (GFP(Ct), Scramble respectively).

## Western blotting

Total proteins were extracted (pools from three 35 mm dishes for each condition) from RAW cells transfected with GFP(Ct) or GFP-ERRα (ERRαWT or ERRαΔAF2) constructs according to the standard methods (Ausubel *et al.* 1996). Western blot analyses were performed using a semidry system. Immunoblotting was performed with anti-GFP (Roche; monoclonal antibody mixture, clones 7.1 and 13.1). Blots were incubated overnight at

**Table 1** Primers and conditions used for PCR

| Gene | Primers | PCR cycles | Temperature (°C) | References |
|---|---|---|---|---|
| *ERRα* | 5′: CAGGAAAGTGAATGCCCAGG<br>3′: CTTTGCAGCAAATATACATT | 24 | 55 | Bonnelye *et al.* (2001) |
| *L32* | 5′: CATGGCTGCCCTCCGGCCTC<br>3′: CATTCTCTTCGCTGCGCTAGCC | 24 | 55 | Bonnelye *et al.* (2001) |
| *EGFP-C1* | 5′: GTGAGCAAGGGCGAGGAGC<br>3′: GGACTTGTACAGCTCGTCC | 25 | 60 | pEGFP-C1 (Clontech) |
| *ERRα1188* | 5′: GTGCACAGAGTCAGAATTGGC | 34 | 55 | NM_007953 |
| *ERRγ* | 5′: ACCATGAATGGCCATCAGAAC<br>3′: ACCAGCTGAGGGTTCAGGTAT | 35 | 59 | Cheung *et al.* (2005) |
| *c-fms* | 5′: TGCTGAAGTGGGAGGGAGAG<br>3′: CTGTAGTCTAAGCATCTGTC | 24 | 55 | BC043054 |
| *OPN* | 5′: GGTGATAGCTTGGCTTATGG<br>3′: CCTCTTCTTTAGTTGACC | 24 | 55 | AF515708 |
| Integrin β3 (*β3*) | 5′: CTTTAAGAAGGAGTGTGTGG<br>3′: GGTCTCATTAAGTCCCC | 28 | 55 | NM_016780 |
| Integrin β1 (*β1*) | 5′: GAGACATGTCAGACCTGCC<br>3′: CCTGAGTAGGATTCATTTTCC | 25 | 55 | BC050906 |
| *Cyclin D1* | 5′: GCTTCTGGTGAACAAGCTC<br>3′: GTGGGCGTGCAGGCCAGACC | 30 | 58 | BC044841 |
| *TRAP* | 5′: TTCCTCCAGGATGGATTCATGG<br>3′: CTGAAGATACTGCAGGTTGTGG | 21 | 55 | NM_007388 |
| *CTR* | 5′: CGAACCTGGTCCAACTATACT<br>3′: CCCTGGAAATGAATCAGAGAG | 28 | 55 | NM_007588 |
| *cytc1* | 5′: ATTTCAACCCTTACTTTCCCG<br>3′: CCACTTATGCCGCTTCATGGC | 24 | 59 | Herzog *et al.* (2006) |
| Integrin β5 (*β5*) | 5′: AGATGAGGTGATCACGTGGG<br>3′: GACAGTGTGTGTGGAGATGG | 29 | 55 | BC058246 |
| Integrin αV (*αv*) | 5′: GCAGATCACCTGCCAGG<br>3′: CTTGCTCTTCTTGAGGTGG | 27 | 55 | NM_008402 |

room temperature with the polyclonal antibody diluted at 1/100, and binding was detected using HRP-conjugated rabbit anti-mice antibodies (1/3000; Bio-Rad Laboratories) and chemiluminescence.

### Immunofluorescence

Cells were fixed in 4% paraformaldehyde, pH 7·2 for 10 min, permeabilized with 0·2% Triton X-100 for 7 min, then incubated with antibodies and Alexa-Fluor-546-Phalloidin as indicated. Cells were imaged with a confocal Zeiss LSM 510, using a X63 (NA 1.4) Plan Neofluor objective. To prevent contamination between fluorochromes, each channel was imaged sequentially, using the multitrack recording module, before merging. Z-cut pictures were obtained using Zeiss LSM 510 software.

### Statistical analysis

Results for the real-time PCR analysis, the quantification of multinucleated TRAP-positive OCs, podosome belt numbers, adhesion, and transmigration were expressed as mean ± s.D., and analyzed statistically by one-way ANOVA with the treatment group as variance

and by Student's *t*-test with InStat software (version 2.01, GraphPad Software, San Diego, CA, USA). Statistical significance was taken as $P < 0.05$ (Student's *t*-tests $*P < 0.05$, $**P < 0.01$, $***P < 0.001$).

## Results

### *ERRα* mRNA expression increased during osteoclast differentiation *in vitro*

Consistent with our previous findings on the presence of ERRα protein in multinucleated TRAP-positive cells in rat femur *in vivo* (Bonnelye *et al.* 2002), we found, by real-time PCR, *ERRα* mRNA expressed throughout all the stages of OC differentiation: in primary leukocytes extracted from spleen (day 0), proliferation (day 2), mononucleated progenitor fusion (day 4), and maturation (days 6–8) with significant increases on days 4–8, when multinucleated OCs were starting to form until they reached maturity (Fig. 1A and B). For comparison, mRNA levels for *ERRβ*, *ERRγ*, and the late OC differentiation marker *CTR* were also assessed (Fig. 1A and B). Interestingly and in contrast to *ERRα*, *ERRγ* mRNA expression decreased dramatically during OC differentiation, while ERRβ was not detected.
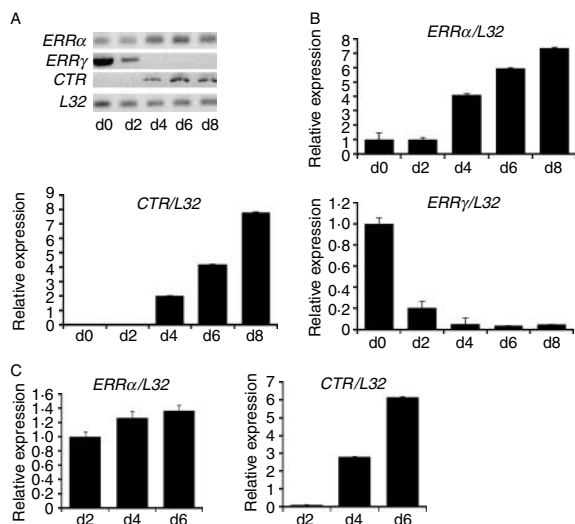
**Figure 1** ERRα is expressed during OC differentiation. (A and B) Real-time PCR showed that ERRα is expressed in leukocytes freshly isolated from murine spleen (d0), as well as during osteoclastogenesis (d6–d8). ERRα and ERRγ expression were normalized against that of the ribosomal protein gene *L32*. For comparison, the mRNA level for *CTR* is also shown. (C) Consistent with primary cells, ERRα is also expressed during OC formation from RAW264.7 cells. d, days in culture.

As previously shown (Bonnelye *et al.* 2002), ERRα is also expressed during OC differentiation of the RAW264.7 macrophage cell line, although fold changes in the expression level are less than that observed in primary OC cultures, which is probably due to the fact that RAW264.7 cells are already committed into the macrophage lineage (Fig. 1C). Given its expression in mature OCs, we then checked whether ERRα was involved in their function.

## Down-regulation of ERRα inhibits OPN and integrin β3 expression in RAW264.7-derived osteoclasts

To check the involvement of ERRα in OC function, we used a truncated version of ERRα lacking the coactivator-binding domain AF2, ERRαΔAF2, which acts as a dominant-negative form of the receptor (Vanacker *et al.* 1999, Bonnelye *et al.* 2007). We first confirmed that GFP-ERRαΔAF2 acts dominant-negatively on the expression of *OPN*, an ERRα target gene in osteoblasts (Vanacker *et al.* 1998, Zirngibl *et al.* 2008, Teyssier *et al.* 2009), in the MC3T3-E1 cell model (Fig. 2A). GFP-ERRαWT was also made and transiently transfected with GFP-ERRαΔAF2 into the RAW264.7 macrophage cell line. Protein size was evaluated by western blotting with a GFP antibody, which detected a protein of ∼80 kDa resulting from the fusion of the GFP (30 kDa) with the ERRαWT protein (around 53 kDa) used as a size control (Fig. 2B). As expected, a band of slightly lower molecular weight was detected in GFP-ERRα

ΔAF2 cells, corresponding to the truncation of the AF2 domain (42 aa; Fig. 2B). Finally, we confirmed the efficacy of GFP-ERRαWT and GFP-ERRαΔAF2 constructs by luciferase reporter assay with a (−448 to −1 bp) BSP promoter fragment (*pGL3BSPLuc*), an ERRα target gene in osteoblasts (Bonnelye *et al.* 2001), in HeLa cells (Fig. 2C). RAW264.7 cells were then stably transfected with the GFP vector alone, which served as control (Ct), and the dominant-negative GFP-ERRα ΔAF2 constructs. Three independent RAW-GFP-ERRα ΔAF2 (1, 2, and 3) and one GFP alone clone were obtained, namely GFP-ΔAF2 (1, 2, and 3) and GFP(Ct) respectively. GFP expression was tested with specific GFP primers after 3 days of culture at the end of the proliferation stage (Fig. 2D and Table 1). *GFP* mRNA expression was observed in GFP(Ct) and all the three stable clones GFP-ΔAF2 (1, 2, and 3), with lower *GFP* expression in GFP-ΔAF2 (1, 2, and 3) versus GFP(Ct) cells (Fig. 2D). As expected, a band of 1·7 kb was amplified with GFP (5′) and ERRα (3′) primers in the RNA isolated from GFP-ΔAF2 (1, 2, and 3) cells, whereas no band was detected in GFP(Ct) cells (Fig. 2D). GFP-ERRαΔAF2 expression was estimated to be tenfold less than the expression of the endogenous ERRα. Moreover, by using a GFP antibody, ERRα was localized by immunofluorescence in mature OCs derived from GFP(Ct) and GFP-ΔAF2 (1, 2, and 3) cells (Fig. 4C and G). As expected, ERRαΔAF2 was detected in both the nucleus and the cytoplasm of GFP-ΔAF2-2-derived OCs (Fig. 4G; similar results were obtained for GFP-ΔAF2-1 and -3), whereas no GFP was detected in the nucleus of GFP(Ct)-derived OCs (Fig. 4C). Also as expected, the expression level of the ERRα target genes, cytochrome *c*-1 (*cytc*; Huss *et al.* 2007) and *OPN*, was significantly reduced in all the three GFP-ΔAF2 clones in comparison with GFP(Ct) cells (Fig. 2E–G), confirming the dominant-negative function of the truncated ERRαΔAF2 construct. Interestingly, the expression of ERRγ, which was expressed at only undetectable to very low levels in RAW264.7 cells, was markedly increased in two of three GFP-ΔAF2 clones in comparison with GFP(Ct) cells (Fig. 2G).

To determine whether ERRα is involved in OC formation, GFP-ΔAF2 (1, 2, and 3) and GFP(Ct) cells were differentiated into mature multinucleated OCs in the presence of M-CSF and RANKL. Based on the cell counts after 3 days of culture, at the end of the proliferation stage, reduction of ERRα transactivation capacity had no effect on cell proliferation (data not shown). Concomitantly, the expression of early markers of OC differentiation, such as TRAP, c-fms, and RANKL (data not shown), and of the proliferation marker cyclin D1 was not affected (Fig. 2E and F). Later during differentiation, while the OPN expression was still down-regulated, we found that integrin β3 chain expression was also decreased in GFP-ΔAF2 (1, 2, and 3)
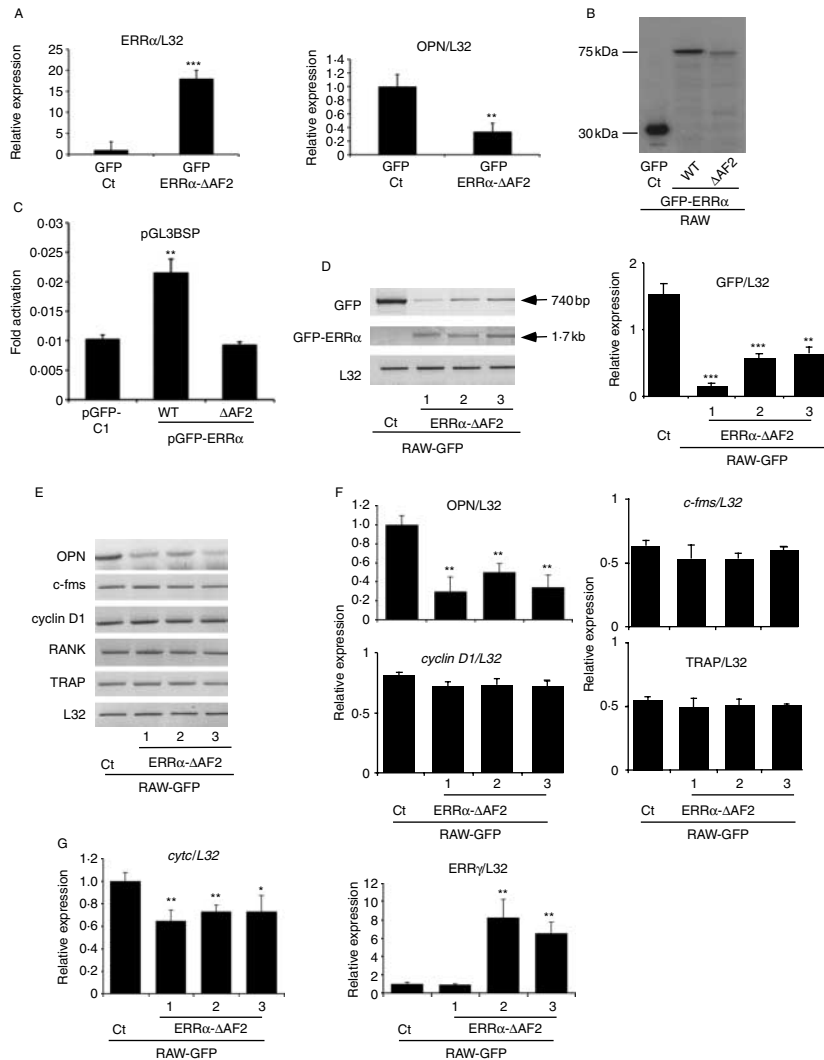
**Figure 2** OPN is down-regulated in RAW cells when ERRα function is disrupted. (A) The MC3T3-E1 osteoblastic cell line was transiently transfected with GFP-ERRαΔAF2, which down-regulated osteopontin expression, confirming that GFP-ERRαΔAF2 acts dominant-negatively (ANOVA, $P=0.0001$ and $P=0.0062$ for GFP-ERRαΔAF2 and OPN expression respectively). (B) RAW264.7 cells were transiently transfected, and overexpression of GFP and GFP-ERRαWT/ΔAF2 after transfection was confirmed by western blotting with a monoclonal antibody against GFP. (C) HeLa cells were cotransfected with a luciferase reporter construct containing a ($-448$ to $-1$ bp) fragment of the mouse BSP (pGL3 mouse BSP) promoter with either empty pEGFP or GFP-ERRαWT/ΔAF2 vectors. As expected, ERRα up-regulated BSP expression, while the ERRαΔAF2 acts dominant-negatively (ANOVA, $P<0.0001$). (D) One clone of RAW264.7 cells stably transfected with pEGFP empty plasmid (GFP(Ct)) and three clones stably transfected with pEGFP-ERRα-ΔAF2 (GFP-ΔAF2) were isolated. GFP expression was assessed, after 3 days of culture, by real-time PCR on triplicate samples and normalized against that of the ribosomal protein gene *L32*. (ANOVA, $P=0.0001$ for GFP in GFP-ΔAF2 (1, 2, and 3) versus GFP(Ct)). (E and F) As expected, OPN expression was decreased (ANOVA, $P=0.0003$ for OPN in GFP-ΔAF2 (1, 2, and 3) versus GFP(Ct)). mRNA expression of the early markers of OC differentiation (*c-fms*, *TRAP*) and proliferation (*cyclin D1*) was not different in GFP-ΔAF2 (1, 2, and 3) cells compared with that in GFP(Ct) cells. (G) *cytc* was down-regulated in GFP-ΔAF2 (1, 2, and 3) versus GFP(Ct) (ANOVA, $P=0.0096$). On the other hand, ERRγ was expressed in two of the GFP-ΔAF2 clones (2, 3) versus GFP(Ct) (ANOVA, $P<0.0001$ for ERRγ).

compared with GFP(Ct) cells (Fig. 3A). On the other hand, the expression of αv, β1 and β5 integrin chain subunits, c-src, CD44, and Traf6 was not affected (Fig. 3A, and data not shown). Moreover, no differences were observed in the expression of OC factors involved in OC fusion (dendritic cell-specific transmembrane protein DC-STAMP (DCS)) or apoptosis (Bcl2 and Bax) in GFP-ΔAF2 (1, 2, and 3)- versus GFP(Ct)-derived OCs (Fig. 3A).

To confirm the putative functional role of ERRα in OC as suggested by the results with the dominant-negative form of ERRαΔAF2, we then checked whether the expression of OPN and integrin β3 chain would be similarly altered by the overexpression of

ERRαWT or by an siRNA directed against ERRα. Transient transfection of ERRαWT in RAW264.7 cells at day 3 (transfection efficiency was very low at earlier stages) up-regulated the expression of OPN and integrin β3 chain at 48 h (Fig. 3B). On the other hand, ERRα siRNA elicited a 60% decrease in the ERRα expression level at day 5 (Fig. 3C). OPN as well as integrin β3 expression was also down-regulated in OCs derived from ERRα siRNA-transfected RAW cells compared with control-transfected cells (Sc). Moreover, ERRγ expression was higher in ERRα siRNA-treated cells (Fig. 3C), consistent with the results in GFP-ΔAF2 (1, 2, and 3)-derived OCs (cf. Fig. 2). Taken together, these data suggest that ERRα does not play a role in the
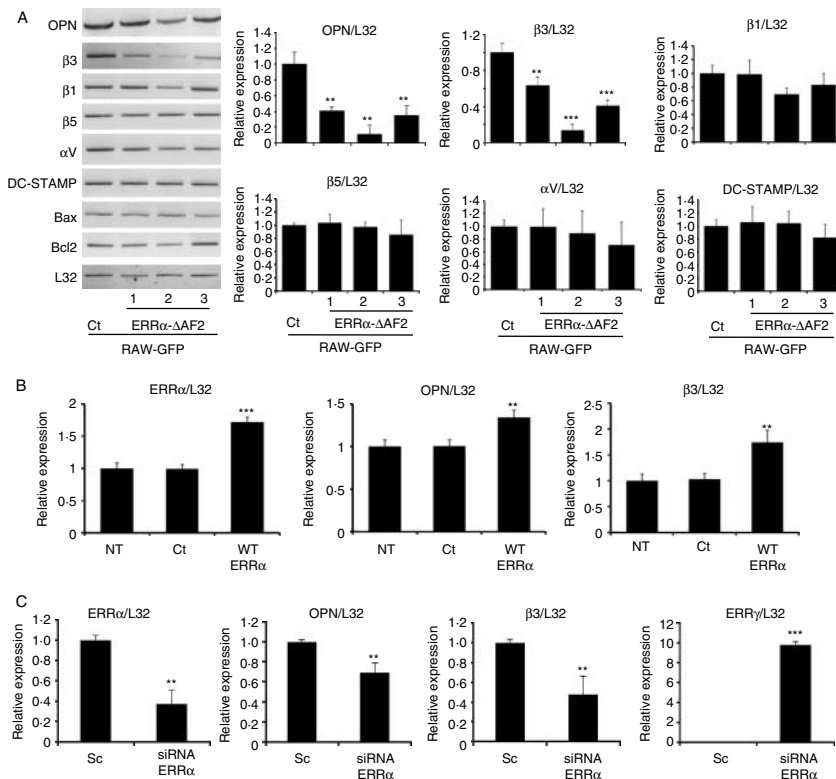


**Figure 3** Implication of ERRα in integrin β3 expression in GFP-ΔAF2-derived OCs (A) Total RNA was extracted from GFP(Ct)- and GFP-ΔAF2 (1, 2, and 3)-derived OCs after 6 days of culture, and real-time PCR was performed on triplicate samples by using primers specific for several genes involved in OCs spreading. Quantification shows a statistically significant decrease in β3 integrin and OPN in GFP-ΔAF2 (1, 2, and 3) (ANOVA, $P=0.0002$; ANOVA, $P=0.0001$, ΔAF2 (1, 2, and 3) versus $C_t$ for OPN and β3 respectively). Markers for adhesion (integrin subunits αv, β1, and β5), OC cell–cell fusion (DC-STAMP) were not modified. (B) Overexpression of ERRα was induced by transient transfection of ERRαWT in RAW264.7 cells. Quantification shows a statistically significant increase in OPN and β3 integrin expression in ERRαWT-transfected cells (ANOVA, $P=0.0001$; ANOVA, $P=0.0011$, $P=0.0023$, for ERRα, OPN, and β3 respectively). (C) siRNA directed against ERRα or a control scrambled siRNA (Sc) was transiently transfected into RAW264.7 cells. As expected, ERRα expression was down-regulated after transfection with ERRα siRNA (ANOVA, $P=0.0015$). Concomitantly, OPN and integrin β3 expression was decreased (ANOVA, $P=0.0053$, $P=0.077$ for OPN and integrin β3 respectively). On the other hand, ERRγ was dramatically expressed in ERRα siRNA-transfected cells versus Sc (ANOVA, $P=0.0004$ for ERRγ).

proliferation/differentiation process of macrophages to OCs, but may be involved in their adhesion, spreading, or migration activities.

## Disruption of ERRα function inhibits OC spreading and formation of podosome belts in RAW264.7-derived osteoclasts

To unravel the function of ERRα in OCs, GFP-ΔAF2 (1, 2, and 3) and GFP(Ct) RAW cells were differentiated into mature multinucleated OCs in the presence of

M-CSF and RANKL. After 6 days, no difference was observed between the number of large multinucleated TRAP-positive OCs and between the nuclei number in GFP-ΔAF2 (1, 2, and 3) versus GFP(Ct) cells, suggesting that ERRα does not affect OC differentiation from macrophages (Fig. 4I–J). However, TRAP-positive GFP-ΔAF2-2-derived OCs (Fig. 4E) appeared less spread than TRAP-positive GFP(Ct)-derived OCs (Fig. 4A). This morphological difference was well correlated to their actin cytoskeletal organization. Indeed, well spread GFP(Ct)-derived OCs exhibited a typical podosome belt (Fig. 4B, D and K), whereas in less spread
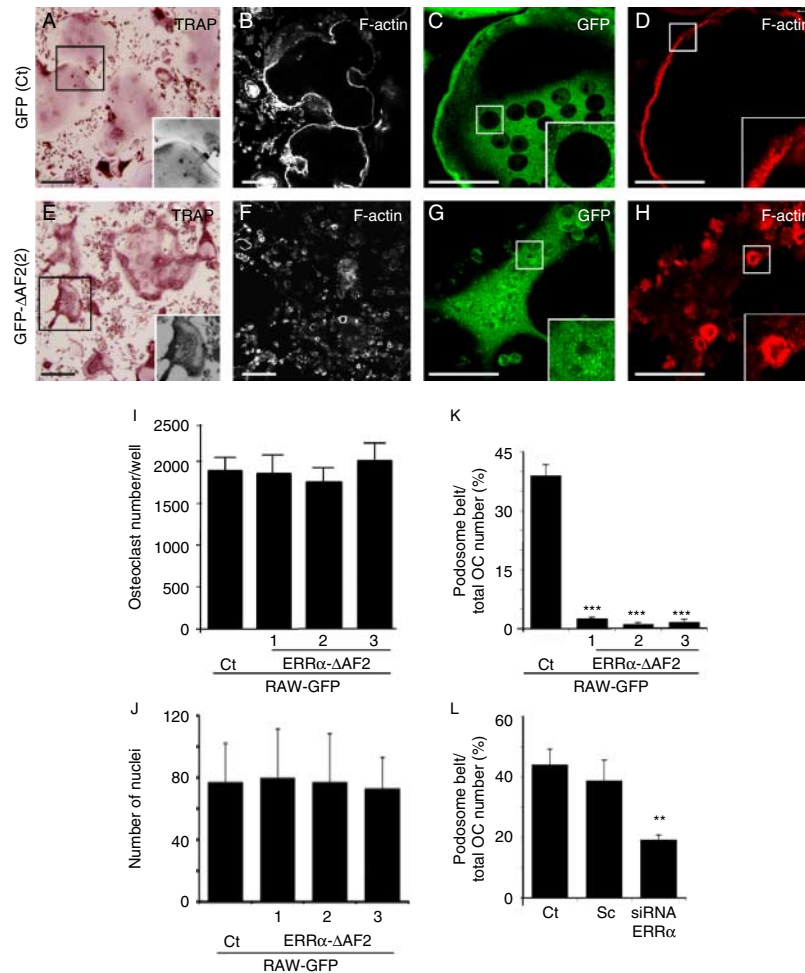


**Figure 4** Involvement of ERRα in OC spreading. RAW-GFP(Ct) and RAW-GFP-ΔAF2 (1, 2, and 3) cells were differentiated for 6 days in culture in the presence of RANKL. (A and E) After TRAP staining, the total number of OCs (I) were quantified. (J) After TRAP staining, the number of nuclei per hundred OCs for each clone was quantified. Podosome belt formation was evaluated after actin staining of (K) GFP(Ct)- and GFP-ΔAF2 (1, 2, and 3)-derived OCs (ANOVA, $P = 0.0001$), or (L) ERRα siRNA or Sc-transfected RAW cell-derived OCs versus non-transfected cells ($C_t$) (ANOVA; $P = 0.0019$). (C and G) Immunolabeling for GFP shows nuclear and cytoplasm location for ERRα. Staining using rhodamine–phalloidin (B, D, F, and H) showed the actin cytoskeletal organization of GFP-ΔAF2 (1, 2, and 3) into actin-containing rings (F and H), while GFP(Ct)-derived OCs exhibited podosome belts (B and D). Bar = 20 μm (A–H). Full color version of this figure available via http://dx.doi.org/10.1677/JME-10-0024.

GFP-ΔAF2 (1, 2, and 3)-derived OCs, podosomes were organized as clusters or small rings (Fig. 4F, H and K). Similar results were obtained in RAW cells transfected with ERRα siRNA versus Sc siRNA or non-transfected cells (Fig. 4L). Together with the down-regulation of both OPN and β3 integrin chain, these latter results strongly suggest that ERRα is involved in OC adhesion.

## Disruption of OC adhesion and transmigration: implication of integrin β3 in GFP-ΔAF2-derived OC

Down-regulation of β3 expression in GFP-ΔAF2-2-derived OCs at day 6 (Fig. 3A) was confirmed by immunofluorescence using an antibody against integrin β3 (Fig. 5A and D). As expected, intense β3 integrin subunit staining was localized around the actin core of podosomes organized in a belt in GFP(Ct)-derived OCs at day 6 (Fig. 5A and B, see merged in Fig. 4C). In contrast, labeling for β3 integrin subunit protein was diffusely distributed within GFP-ΔAF2-2-derived OCs at day 6 (Fig. 5D and E, see merged in F). Since we, and others, have shown the importance of c-src in integrin signaling for actin organization, we looked for phosphorylated c-src localization in OCs expressing the dominant-negative form of ERRα. Whereas phosphorylated c-src was distributed around the podosome belt in GFP(Ct)-derived OCs on day 6 (Fig. 5G and H, see merged in I), it was diffusely
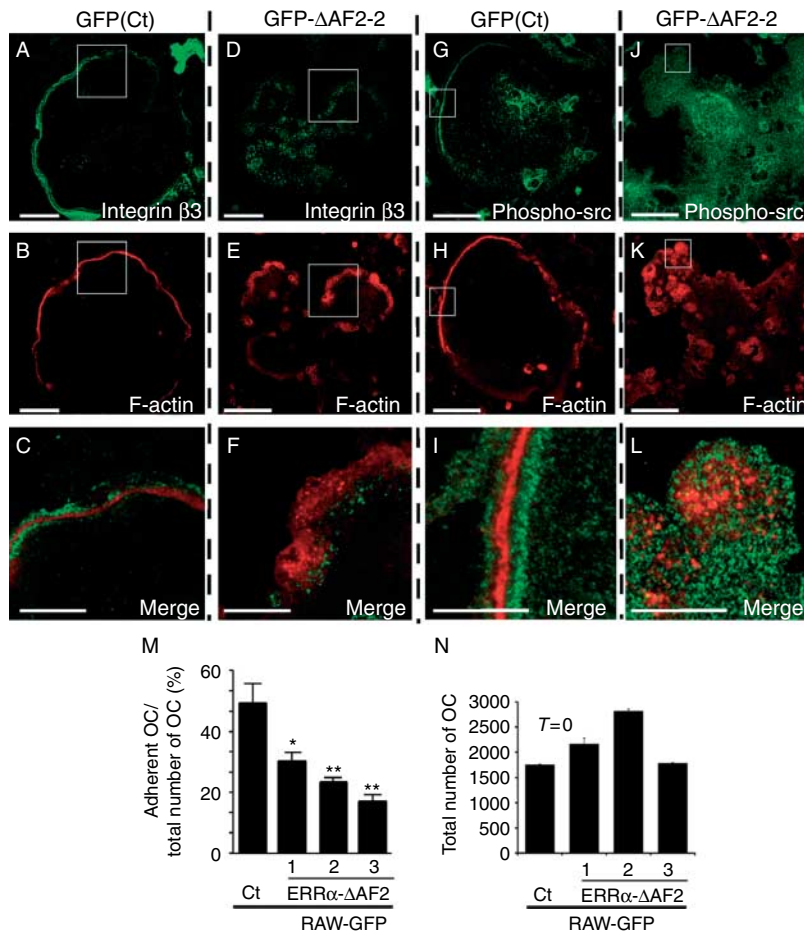


**Figure 5** Integrin subunit β3 expression and localization are altered in GFP-ΔAF2-derived OCs. (A–L) β3 integrin subunit (A, D, C, and F in green), phosphorylated c-src (G, J, I, and L in green), and actin (B, C, E, F, H, I, K, and L in red) were immunostained in control (A–C; G–I) and in GFP-ΔAF2-2-derived OCs (D–F; J–L). Whereas control OC formed typical podosome belts with actin dots surrounded by β3 integrin and phosphorylated c-src (A–C; G–I), podosomes of GFP-ΔAF2-2-derived OCs were disorganized with mislocalized β3 integrin and phosphorylated c-src (D–F; J–L). Merged images of the closeup areas of actin, β3, and phosphorylated c-src respectively are also shown (C, F, I, and L). Bar = 20 μm. (M) Adhesion ability was also evaluated (ANOVA, $P = 0.0001$; ΔAF2 (1, 2, and 3)), while (N) OC viability was evaluated by counting the total number of OCs used in the adhesion test at $T = 0$.

localized in GFP-ΔAF2-2 cells (Fig. 5J and K, see merged in L). Similarly, vinculin localization was disrupted in GFP-ΔAF2 cells (data not shown) compared with GFP(Ct)-derived OCs at day 6. These results suggest that disturbing ERRα function impairs a signaling pathway linked to OPN, integrin β3, activated c-src, and actin organization. Moreover, and in agreement with the decrease in mature OC spreading, we observed a decrease in OC adhesion in GFP-ΔAF2 (1, 2, and 3)-derived OCs compared with GFP(Ct)-derived cells (by 40% in ΔAF2-1, 50% in ΔAF2-2, and 68% in ΔAF2-3 compared with GFP(Ct); Fig. 5M). It was observed that the differences in OC viability, as reflected by OC number, cannot account for the differences in spreading between GFP(Ct)- and GFP-ΔAF2 (1, 2, and 3)-derived OCs ($T=0$; Fig. 5N).

To address further the consequences of disrupting the actin structure due to the expression of a dominant-negative form of ERRα in OCs, we then checked whether OC transmigration was affected (Saltel *et al.* 2006). To this end, mature GFP-ΔAF2 (1, 2, and 3)- and GFP(Ct)-derived OCs were seeded onto confluent osteoblastic MC3T3-E1 cells. After 20 min, large rounded OCs (identified by GFP expression in green, white arrows) derived from GFP-ΔAF2 (1, 2, and 3) (Fig. 6G, see Z-cut section E) and GFP(Ct) (Fig. 6C, see Z-cut section A) cells were localized on the top of confluent osteoblastic MC3T3-E1 cell layers (red, see white asterisk). After 12 h, OCs derived from GFP(Ct) cells were well spread and attached to the substratum beneath the osteoblasts (Fig. 6D, and Z-cut section in B), showing that they had transmigrated through the MC3T3-E1 cell layers. In contrast, after 12 h of culture, OCs derived from GFP-ΔAF2-2 cells appeared 'frozen' on the top of the MC3T3-E1 cell layers where they maintained a rounded shape (Fig. 6H, see GFP-positive OCs (white arrow) and Z-cut section in Fig. 6F). Similar observations were obtained for GFP-ΔAF2 clones 1 and 3
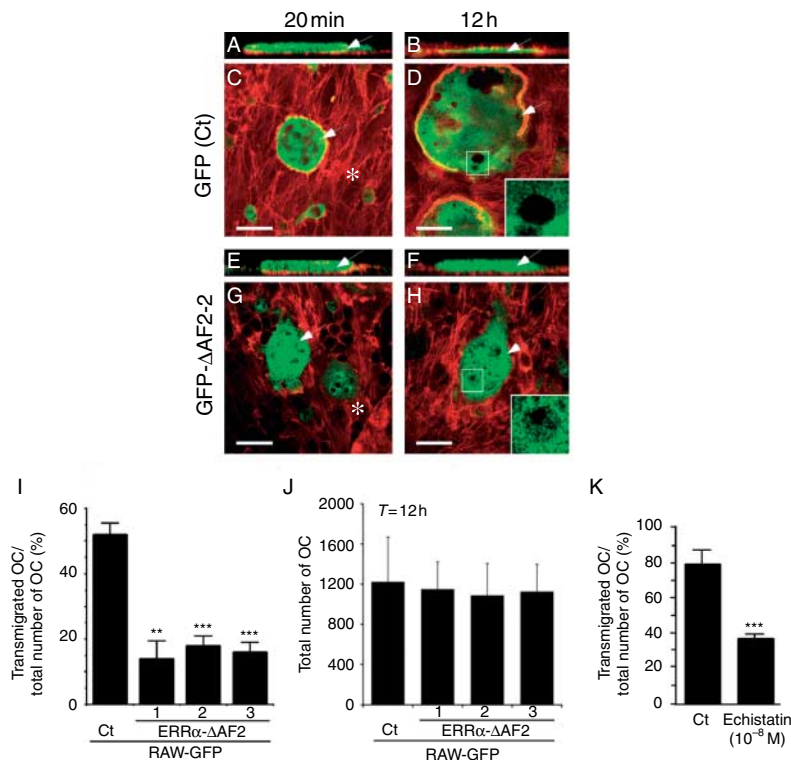


**Figure 6** Transmigration ability is decreased in GFP-ΔAF2-derived OCs. GFP(Ct) (A–D, green) and GFP-ΔAF2-2-derived OCs (E–H, green) were seeded on the top of MC3T3-E1 cells (red). Z-cut sections show that 20 min after seeding, OCs were lying on the top of MC3T3-E1 cells (A and E). Control OCs had transmigrated down through the osteoblast layer 12 h after seeding (B), whereas GFP-ΔAF2-derived OCs had not (F). (I) Inhibition of transmigration in GFP-ΔAF2 (1, 2, and 3)- versus GFP(Ct)-derived OCs was quantified. (J) OC viability was evaluated by counting the total number of OCs used in the transmigration assay. (K) Inhibition of transmigration was also observed when mature OCs were treated with echistatin. (I and K) Results represent the mean (%) of the transmigrated OC/total OC number ± s.d. for triplicate determinations. (I) ANOVA; $P=0·001$. (K) ANOVA; $P=0·0004$. Bar = 20 μm.

(data not shown). Quantification of transmigrated OCs versus non-transmigrated OCs confirmed a significant decrease (72% in ΔAF2-1, 63% in ΔAF2-2, and 67% in ΔAF2-3) in the transmigrated OC numbers in GFP-ΔAF2 (1, 2, and 3)- compared with GFP(Ct)-derived OCs (Fig. 6I). Viability of the transmigrated GFP(Ct)- and GFP-ΔAF2 (1, 2, and 3)-derived OCs is equivalent (total OC number at $T=12$ h; Fig 6J). Interestingly, the inhibition of transmigration observed with the knock-down of ERRα correlated with that observed after blocking integrins with echistatin, an RGD disintegrin, in primary OCs re-seeded onto confluent osteoblastic MC3T3-E1 cells (Fig. 6K).

## Discussion

We report that the overexpression or knockdown of ERRα function in the RAW264.7 macrophage cell line either by stable transfection of a dominant-negative form of ERRα, GFP-ERRαΔAF2 or by ERRα siRNA leads to modulation of the expression of OPN and β3 integrin subunit with concomitant actin cytoskeletal disorganization in the podosome belt, reduced adhesion on tissue culture plastic or glass, and reduced transmigration activity. Although *ERRα* knockout mice and cells are now available, our work was initiated when these were not available, and both our stable and transient knockdown approaches gave comparable and highly reproducible results. It is therefore not clear why no detectable alteration in the OC parameters was observed in *ERRα* knockout mice (Delhon *et al.* 2009, Teyssier *et al.* 2009), but it seems likely that compensatory mechanisms involving ERRγ may be operating, since we found that ERRγ is expressed in RAW264.7 cells when ERRα function is disrupted.

The molecular basis for the ERRα effect on cell mobility is of interest because *OPN*, which is expressed in several motile cell types including OCs and many tumor cell lines (Standal *et al.* 2004), has been described as a target gene of ERRα in promoter reporter assays *in vitro* (Vanacker *et al.* 1998, Zirngibl *et al.* 2008). OPN is involved in cell adhesion and migration and promotes cell attachment to bone (Denhardt & Noda 1998). Adhesion receptors αvβ1, αvβ3, and αvβ5 integrins and the hyaluronan receptor (CD44) are all receptors for OPN, and their interactions are crucial for OC adhesion and motility (McHugh *et al.* 2000, Chellaiah & Hruska 2003). Notably, OPN is known to stimulate glass-adherent OC migration through the αvβ3 integrin-induced activation of c-src and actin cytoskeletal reorganization into podosome belts (Duong *et al.* 1998). While αv, β1, and β5 integrin subunits and CD44 were not affected by the changes in ERRα activity, the expression of the β3 integrin subunit was down-regulated in siRNA and

GFP-ΔAF2-derived OCs. In addition, more detailed studies in GFP-ΔAF2-derived OCs showed that the disruption of podosome belt formation was accompanied by an aberrant/diffuse distribution of the β3 integrin subunit, activated c-src, and vinculin. Thus, it is likely that the inhibition of adhesion and disruption of the podosome belt observed in GFP-ΔAF2-derived OCs is a consequence of the reduced expression of both OPN and β3 that consequently induced the disrupted localization of activated c-src. Moreover, although neither of the latter is known to be involved in OC transmigration, the fact that αvβ3 is involved in monocyte transendothelial migration, that echistatin, an RGD disintegrin, induces a decrease in OC transmigration, and that c-src is involved in OC transmigration through MC3T3-E1 cell layers suggests that the β3 integrin subunit may be involved in OC transmigration (Weerasinghe *et al.* 1998, Saltel *et al.* 2006). Indeed, in the presence of PP2, a c-src inhibitor, OCs maintain a rounded shape and sit on the top of MC3T3-E1 cell layers (Saltel *et al.* 2006) in a manner similar to GFP-ΔAF2-derived OCs. These data suggest that the disruption of activated c-src localization may, at least in part, be due to down-regulated OPN and/or integrin subunit β3 expression and may be responsible for the inhibition of transmigration in GFP-ΔAF2-derived OCs.

We have previously shown that ERRα positively regulates osteoblast formation in rat calvarial cells *in vitro*, acting at multiple developmental times to regulate both proliferation and differentiation events (Bonnelye *et al.* 2001). However, more recent data with *ERRα* knockout mice and with human bone marrow stromal cells suggest that ERRα may play a negative regulatory role in other models or at other developmental times (Delhon *et al.* 2009, Teyssier *et al.* 2009). Further complicating the issue, one study suggests that an *ESRRA* gene regulatory variant leading to increased ERRα expression is associated with increased bone mineral density in premenopausal women (Laflamme *et al.* 2005), although a recent report has failed to confirm the observation (Giroux *et al.* 2008). Such apparently complex and multiphasic activities, complicated by potential compensatory mechanisms involving other ERR family members, are in keeping with our current data showing that down-regulation of ERRα decreases OC transmigration, suggesting that ERRα may positively regulate OC migration. Altogether, the data suggest that ERRα may contribute to bone homeostasis not only through effects on osteoblast lineage cells but also on OCs.

ERRα expression in other highly motile cells such as dendritic cells and macrophages (Sonoda *et al.* 2007, Bonnelye *et al.* 2008) supports a role for ERRα in inflammatory diseases associated with osteoclastic bone degradation such as rheumatoid arthritis and other

diseases, where αvβ3 and OPN are also implicated (Wilder 2002, Yumoto *et al.* 2002). In this regard, recently, and similarly to our data on OC migration, siRNA-mediated knockdown of ERRα in the highly aggressive breast carcinoma MDA-231 cell line resulted in a dramatic decrease in their migration (Stein *et al.* 2008). We thus hypothesize that the ERRα-regulated OPN and integrin subunit β3 pathway that we described here may also be operative in cancer cells.

In conclusion, ERRα is expressed in OCs where it regulates the expression of OPN and integrin subunit β3, and plays a role in the spreading, organization, and/or stabilization of podosomes at the cell periphery, as well as in the adhesion and transmigration in a RAW cell culture model *in vitro*. Further understanding of the mechanisms by which ERRα modulates migration in the normal development and disease is required. In the meantime, our data suggest that the regulation of ERRα activity may provide a new therapeutic strategy for inflammatory and bone diseases associated with an imbalance in bone remodeling due to excessive OC resorption.

## Declaration of interest

## Funding

## Acknowledgements

## References

Ausubel FM, Brent R, Kinston RE, Moore DD, Seidman JG, Smith JA & Struhl K 1996 *Current Protocols in Molecular Biology*, vol 1, unit 10.8. New York, NY: John Wiley & Sons.

Benoit G, Cooney A, Giguere V, Ingraham H, Lazar M, Muscat G, Perlmann T, Renaud JP, Schwabe J, Sladek F *et al.* 2006 International Union of Pharmacology. LXVI. Orphan nuclear receptors. *Pharmacological Reviews* **58** 798–836. (doi:10.1124/pr.58.4.10)

Bonnelye E, Merdad L, Kung V & Aubin JE 2001 The orphan nuclear estrogen receptor-related receptor (ERR) is expressed throughout osteoblast differentiation and regulates bone formation *in vitro*. *Journal of Cell Biology* **153** 971–983. (doi:10.1083/jcb.153.5.971)

Bonnelye E, Kung V, Laplace C, Galson DL & Aubin JE 2002 Estrogen receptor-related receptor α impinges on the estrogen axis in bone: potential function in osteoporosis. *Endocrinology* **143** 3658–3670. (doi:10.1210/en.2002-220095)

Bonnelye E, Zirngibl RA, Jurdic P & Aubin JE 2007 The orphan nuclear estrogen receptor-related receptor-α regulates cartilage formation *in vitro*: implication of Sox9. *Endocrinology* **148** 1195–1205. (doi:10.1210/en.2006-0962)

Bonnelye E, Laurin N, Jurdic P, Hart DA & Aubin JE 2008 Estrogen receptor-related receptor-α (ERR-α) is dysregulated in inflammatory arthritis. *Rheumatology* **47** 1785–1791. (doi:10.1093/rheumatology/ken368)

Boyle WJ, Simonet WS & Lacey DL 2003 Osteoclast differentiation and activation. *Nature* **423** 337–342. (doi:10.1038/nature01658)

Chabadel A, Banon-Rodriguez I, Cluet D, Rudkin BB, Wehrle-Haller B, Genot E, Jurdic P, Anton IM & Saltel F 2007 CD44 and β3 integrin organize two functionally distinct actin-based domains in osteoclasts. *Molecular Biology of the Cell* **18** 4899–4910. (doi:10.1091/mbc.E07-04-0378)

Chellaiah MA & Hruska KA 2003 The integrin α(v)β(3) and CD44 regulate the actions of osteopontin on osteoclast motility. *Calcified Tissue International* **72** 197–205. (doi:10.1007/s00223-002-1025-6)

Cheung CP, Yu S, Wong KB, Chan LW, Lai FM, Wang X, Suetsugi M, Chen S & Chan FL 2005 Expression and functional study of estrogen receptor-related receptors in human prostatic cells and tissues. *Journal of Clinical Endocrinology and Metabolism* **90** 1830–1844. (doi:10.1210/jc.2004-1421)

Delaisse JM, Andersen TL, Engsig MT, Henriksen K, Troen T & Blavier L 2003 Matrix metalloproteinases (MMP) and cathepsin K contribute differently to osteoclastic activities. *Microscopy Research and Technique* **61** 504–513. (doi:10.1002/jemt.10374)

Delhon I, Gutzwiller S, Morvan F, Rangwala S, Wyder L, Evans G, Studer A, Kneissel M & Fournier B 2009 Absence of estrogen receptor related α increases osteoblastic differentiation and cancellous bone mineral density. *Endocrinology* **150** 4463–4472. (doi:10.1210/en.2009-0121)

Denhardt DT & Noda M 1998 Osteopontin expression and function: role in bone remodeling. *Journal of Cellular Biochemistry. Supplement* **30–31** 92–102. (doi:10.1002/(SICI)1097-4644(1998)72:30/31+<92::AID-JCB13>3.0.CO;2-A)

Destaing O, Saltel F, Geminard JC, Jurdic P & Bard F 2003 Podosomes display actin turnover and dynamic self-organization in osteoclasts expressing actin-green fluorescent protein. *Molecular Biology of the Cell* **14** 407–416. (doi:10.1091/mbc.E02-07-0389)

Domon T, Yamazaki Y, Fukui A, Ohnishi Y, Takahashi S, Yamamoto T & Wakita M 2002 Three-dimensional distribution of the clear zone of migrating osteoclasts on dentin slices *in vitro*. *Tissue and Cell* **34** 326–336. (doi:10.1016/S0040816600000137)

Duong LT, Lakkakorpi PT, Nakamura I, Machwate M, Nagy RM & Rodan GA 1998 PYK2 in osteoclasts is an adhesion kinase, localized in the sealing zone, activated by ligation of α(v)β3 integrin, and phosphorylated by src kinase. *Journal of Clinical Investigation* **102** 881–892. (doi:10.1172/JCI3212)

Gennari L, De Paola V, Merlotti D, Martini G & Nuti R 2007 Steroid hormone receptor gene polymorphisms and osteoporosis: a pharmacogenomic review. *Expert Opinion on Pharmacotherapy* **8** 537–553. (doi:10.1517/14656566.8.5.537)

Giguere V, Yang N, Segui P & Evans RM 1988 Identification of a new class of steroid hormone receptors. *Nature* **331** 91–94. (doi:10.1038/331091a0)

Giroux S, Elfassihi L, Cole DE & Rousseau F 2008 Replication of associations between women LRP5 and ESRRA variants and bone density in premenopausal women. *Osteoporosis International* **19** 1769–1775. (doi:10.1007/s00198-008-0617-z)

Green S, Walter P, Kumar V, Krust A, Bornert JM, Argos P & Chambon P 1986 Human oestrogen receptor cDNA: sequence, expression and homology to v-erb-A. *Nature* **320** 134–139. (doi:10.1038/320134a0)

Greschik H, Wurtz JM, Sanglier S, Bourguet W, van Dorsselaer A, Moras D & Renaud JP 2002 Structural and functional evidence for ligand-independent transcriptional activation by the estrogen-related receptor 3. *Molecular Cell* **9** 303–313. (doi:10.1016/S1097-2765(02)00444-6)

Herzog B, Cardenas J, Hall RK, Villena JA, Budge PJ, Giguère V, Granner DK & Kralli A 2006 Estrogen-related receptor alpha is a repressor of phosphoenolpyruvate carboxykinase gene transcription. *Journal of Biological Chemistry* **281** 99–106. (doi:10.1074/jbc.M509276200)

Huss JM, Imahashi K, Dufour CR, Weinheimer CJ, Courtois M, Kovacs A, Giguere V, Murphy E & Kelly DP 2007 The nuclear receptor ERRα is required for the bioenergetic and functional adaptation to cardiac pressure overload. *Cell Metabolism* **6** 25–37. (doi:10.1016/j.cmet.2007.06.005)

Jurdic P, Saltel F, Chabadel A & Destaing O 2006 Podosome and sealing zone: specificity of the osteoclast model. *European Journal of Cell Biology* **85** 195–202. (doi:10.1016/j.ejcb.2005.09.008)

Kallen J, Schlaeppi JM, Bitsch F, Filipuzzi I, Schilb A, Riou V, Graham A, Strauss A, Geiser M & Fournier B 2004 Evidence for ligand-independent transcriptional activation of the human estrogen-related receptor α (ERRα): crystal structure of ERRα ligand binding domain in complex with peroxisome proliferator-activated receptor coactivator-1α. *Journal of Biological Chemistry* **279** 49330–49337. (doi:10.1074/jbc.M407999200)

Kuiper GG, Enmark E, Pelto-Huikko M, Nilsson S & Gustafsson JA 1996 Cloning of a novel receptor expressed in rat prostate and ovary. *PNAS* **93** 5925–5930. (doi:10.1073/pnas.93.12.5925)

Laflamme N, Giroux S, Loredo-Osti JC, Elfassihi L, Dodin S, Blanchet C, Morgan K, Giguere V & Rousseau F 2005 A frequent regulatory variant of the estrogen-related receptor α gene associated with BMD in French–Canadian premenopausal women. *Journal of Bone and Mineral Research* **20** 938–944. (doi:10.1359/JBMR.050203)

Luo J, Sladek R, Carrier J, Bader JA, Richard D & Giguere V 2003 Reduced fat mass in mice lacking orphan nuclear receptor estrogen-related receptor α. *Molecular and Cellular Biology* **23** 7947–7956. (doi:10.1128/MCB.23.22.7947-7956.2003)

McHugh KP, Hodivala-Dilke K, Zheng MH, Namba N, Lam J, Novack D, Feng X, Ross FP, Hynes RO & Teitelbaum SL 2000 Mice lacking β3 integrins are osteosclerotic because of dysfunctional osteoclasts. *Journal of Clinical Investigation* **105** 433–440. (doi:10.1172/JCI8905)

Saltel F, Destaing O, Bard F, Eichert D & Jurdic P 2004 Apatite-mediated actin dynamics in resorbing osteoclasts. *Molecular Biology of the Cell* **15** 5231–5241. (doi:10.1091/mbc.E04-06-0522)

Saltel F, Chabadel A, Zhao Y, Lafage-Proust MH, Clezardin P, Jurdic P & Bonnelye E 2006 Transmigration: a new property of mature multinucleated osteoclasts. *Journal of Bone and Mineral Research* **21** 1913–1923. (doi:10.1359/jbmr.060821)

Saltel F, Chabadel A, Bonnelye E & Jurdic P 2008 Actin cytoskeletal organisation in osteoclasts: a model to decipher transmigration and matrix degradation. *European Journal of Cell Biology* **87** 459–468. (doi:10.1016/j.ejcb.2008.01.001)

Sonoda J, Laganiere J, Mehl IR, Barish GD, Chong LW, Li X, Scheffler IE, Mock DC, Bataille AR, Robert F *et al.* 2007 Nuclear receptor ERRα and coactivator PGC-1 β are effectors of IFN-γ-induced host defense. *Genes and Development* **21** 1909–1920. (doi:10.1101/gad.1553007)

Standal T, Borset M & Sundan A 2004 Role of osteopontin in adhesion, migration, cell survival and bone remodeling. *Experimental Oncology* **26** 179–184.

Stein RA, Chang CY, Kazmin DA, Way J, Schroeder T, Wergin M, Dewhirst MW & McDonnell DP 2008 Estrogen-related receptor α is critical for the growth of estrogen receptor-negative breast cancer. *Cancer Research* **68** 8805–8812. (doi:10.1158/0008-5472.CAN-08-1594)

Teitelbaum SL 2007 Osteoclasts: what do they do and how do they do it? *American Journal of Pathology* **170** 427–435. (doi:10.2353/ajpath.2007.060834)

Teyssier C, Gallet M, Rabier B, Monfoulet L, Dine J, Macari C, Espallergues J, Horard B, Giguère V, Cohen-Solal M *et al.* 2009 Absence of ERRα in female mice confers resistance to bone loss induced by age or estrogen-deficiency. *PLoS ONE* **4** e7942. (doi:10.1371/journal.pone.0007942)

Vaananen HK, Zhao H, Mulari M & Halleen JM 2000 The cell biology of osteoclast function. *Journal of Cell Science* **113** 377–381.

Vanacker JM, Delmarre C, Guo X & Laudet V 1998 Activation of the osteopontin promoter by the orphan nuclear receptor estrogen receptor related α. *Cell Growth and Differentiation* **9** 1007–1014.

Vanacker JM, Bonnelye E, Chopin-Delannoy S, Delmarre C, Cavailles V & Laudet V 1999 Transcriptional activities of the orphan nuclear receptor ERRα (estrogen receptor-related receptor-α). *Molecular Endocrinology* **13** 764–773. (doi:10.1210/me.13.5.764)

Weerasinghe D, McHugh KP, Ross FP, Brown EJ, Gisler RH & Imhof BA 1998 A role for the αvβ3 integrin in the transmigration of monocytes. *Journal of Cell Biology* **142** 595–607. (doi:10.1083/jcb.142.2.595)

Wilder RL 2002 Integrin αVβ3 as a target for treatment of rheumatoid arthritis and related rheumatic diseases. *Annals of Rheumatic Disease* **61** (Supplement 2) ii96–ii99. (doi:10.1136/ard.61.suppl_2.ii96)

Yumoto K, Ishijima M, Rittling SR, Tsuji K, Tsuchiya Y, Kon S, Nifuji A, Uede T, Denhardt DT & Noda M 2002 Osteopontin deficiency protects joints against destruction in anti-type II collagen antibody-induced arthritis in mice. *PNAS* **99** 4556–4561. (doi:10.1073/pnas.052523599)

Zirngibl RA, Chan JS & Aubin JE 2008 Estrogen receptor-related receptor α (ERRα) regulates osteopontin expression through a non-canonical ERRα response element in a cell context-dependent manner. *Journal of Molecular Endocrinology* **40** 61–73. (doi:10.1677/JME-07-0114)